



5th International Conference on Functional Materials & Devices (ICFMD 2015)

## Comparison on electrochemical performances of $\text{LiNi}_{0.5}\text{Mn}_{1.5}\text{O}_4$ cathode materials synthesized using different precursors

Nabilah Mokhtar and Nurul Hayati Idris\*

*School of Ocean Engineering, Universiti Malaysia Terengganu, 21030 Kuala Terengganu, Malaysia*

---

### Abstract

In this work,  $\text{LiNi}_{0.5}\text{Mn}_{1.5}\text{O}_4$  has been synthesized by using acetate and carbonate precursors, respectively and ball-milled with citric acid, followed by heat treatment at high temperature. The structure, morphology and electrochemical performances of all samples were investigated using X-ray diffraction, scanning electron microscope, and galvanostatic testing. The high crystallinity and small particle size are affected by the homogeneity of the samples with the presence of citric acid. It was shown that the electrochemical performances of  $\text{LiNi}_{0.5}\text{Mn}_{1.5}\text{O}_4$  prepared from acetate precursor exhibit the highest discharge capacity of 120 mAh  $\text{g}^{-1}$  at 1 C rate.

© 2016 The Authors. Published by Elsevier Ltd. This is an open access article under the CC BY-NC-ND license (<http://creativecommons.org/licenses/by-nc-nd/3.0/>).

Selection and Peer-review under responsibility of Conference Committee Members of 5th International Conference on Functional Materials & Devices (ICFMD 2015).

*Keywords:* Lithium-ion batteries; Lithium nickel manganese oxide; Cathode; Specific capacity

---

### 1. Introduction

Due to the increasing demand for high energy storage, environmental issue, safety and energy crisis, increasing number of research have been developed to solve the issues. Li-ion battery has become one of the potential candidates to overcome the issues due to its high energy density and excellent cycling performances. Various

---

\* Corresponding author. Tel.: +6096683185; Fax: +6096683391 .  
E-mail address: [nurulhayati@umt.edu.my](mailto:nurulhayati@umt.edu.my)

cathode materials have been introduced and commercialized such as  $\text{LiCoO}_2$  [1, 2],  $\text{LiMn}_2\text{O}_4$  [3], and  $\text{LiFePO}_4$  [4], however, due to some limitations of these materials such as expensive, toxic and low operating voltage, other alternatives of cathode materials are being explored [5].  $\text{LiNi}_{0.5}\text{Mn}_{1.5}\text{O}_4$  (LNMO) have received attentions due to high working voltage of 4.7 V, low cost, and shows a big difference in high energy density about 20% and 30% when compared with  $\text{LiCoO}_2$  and  $\text{LiFePO}_4$ , respectively [6, 7]. In addition, with an appropriate anode, LNMO in full cell shows an attractive operating voltage of  $\sim 3.4$  V [8]. However, there are some obstacles in preparing pure LNMO including the presence of rock salt phase such as  $\text{Li}_x\text{Ni}_{1-x}\text{O}$  and  $\text{NiO}$ . In addition, the disproportionation reaction of  $\text{Mn}^{3+}$  will cause the dissolution of  $\text{Mn}^{2+}$  and the separation of particle from Jahn-Teller distortion during intercalation/deintercalation processes could influence the cycling performances of LNMO. Various methods to synthesize LNMO have been developed to overcome these problems such as sol-gel [9], combustion [10], coprecipitation [11] emulsion drying [12] and polymer precursor [13] methods and substitution with other cations such as Ru [14], Mg [15], Cr [16] and Al [17]. Although these approaches have been shown to prevent the formation of impurity, but it consumes high cost and complicated synthetic route [18]. Therefore, simple method of using ball-mill and mixing the precursor with chelating agent such as citric acid could control the morphology and expected to give homogeneity of LNMO phase which in results, provide a better electrochemical performances. The presence of citric acid have been shown to give significant effect on phase purity, and good stoichiometric inorganic oxides, thus give better performance of the material [19]. On the other hand, citric acid could assist the dispersion of precursor into molecular level in the solution [20]. Also, the decomposition of citric acid during sintering process could reduce the particle size, shorter the diffusion path of  $\text{Li}^+$  and beneficial to the extraction and insertion of  $\text{Li}^+$ , which in turn, improve the electrochemical performance of the powder [20, 21]. Herein, by using two different LNMO precursors which are acetate and carbonate, respectively, LNMO will be synthesized by using a simple mechanical ball-milling with the addition of chelating agent. To the best of our knowledge, there is no report on this approach in synthesizing LNMO powder. The phase, morphology and electrochemical performances of the as-prepared LNMO are systematically investigated.

## 2. Experimental

### 2.1. Materials preparation

LNMO samples were prepared by mechanical ball milling using two different starting precursors namely, acetate and carbonate precursors. For LNMO synthesized using acetate precursors,  $\text{C}_4\text{H}_6\text{MnO}_4 \cdot 4\text{H}_2\text{O}$ ,  $\text{C}_4\text{H}_6\text{NiO}_4 \cdot 4\text{H}_2\text{O}$ , and  $\text{C}_2\text{H}_3\text{LiO}_2 \cdot \text{H}_2\text{O}$  were ball-milled together with 50 wt. % citric acid for 2 h at 300 rpm. Similar method was adopted to prepare LNMO using carbonate precursor;  $\text{MnCO}_3$ ,  $\text{C}_2\text{H}_6\text{Ni}_5\text{O}_{12} \cdot 4\text{H}_2\text{O}$ , and  $\text{Li}_2\text{CO}_3$ . Then, the mixture were annealed at 350 °C for 5 h, followed by a thermal treatment at 750 °C, 850 °C and 950 °C for 12 h in air, respectively. The synthesized powders obtained from acetate precursors are labeled as A350, A750, A850, and A950 and powders obtained from carbonate precursors are marked as C350, C750, C850, and C950.

### 2.2. Materials characterization

The structure and phase of LNMO was determined by X-ray Diffraction (XRD) (Shimadzu) with  $\text{Cu K}\alpha$  radiation and wavelength 1.5418 Å. The analysis was performed between 5° and 80° at a scan rate of 2°  $\text{min}^{-1}$  and step size of 0.02°. The morphology and particle size of the sample was characterized using scanning electron microscopy (SEM) (JEOL JSM-6360LA).

### 2.3. Electrochemical Characterization.

For the electrode preparation, 75 wt. % of LNMO, 20 wt. % of carbon black, and 5 wt. % of carboxymethyl cellulose (CMC) as binder were dissolved in deionized water. Then, the homogenous slurry was paste onto aluminium foil (geometrical area: 1 × 1 cm) and dried at 100 °C under vacuum. The weight of the active material on each electrode was  $\sim 1.5$  mg. The coin cell type (CR2032) was assembled in Argon filled glove-box with lithium metal as counter electrode and polypropylene as separator. 1 M  $\text{LiPF}_6$  in a mixture of ethylene carbonate (EC) and

dimethyl carbonate (DMC) was used as an electrolyte. The galvanostatic charge-discharge was tested at a potential ranging from 3.0 to 4.9 V at 1 C rate ( $1\text{ C} = 147\text{ mA g}^{-1}$ ). The cyclic voltammetry (CV) test was performed using CH Instruments (CHI760e) at a scan rate of  $0.5\text{ mV s}^{-1}$ .

### 3. Results and Discussion

The XRD patterns of all samples are shown in Fig. 1 and 2. All peaks are fitted well with the spinel cubic structure with space group of  $Fd-3m$  (JCPDS card no.: 80-2162). It is also can be seen the presence of small peaks of rock salt phase NiO as an impurity at  $37.29^\circ$ ,  $43.34^\circ$ ,  $62.91^\circ$ ,  $75.46^\circ$ , and  $79.38^\circ$  (JCPDS Card no.: 73-1523). The presence of NiO can be attributed to oxygen deficiency during synthesis of LNMO [22]. Clearly, the intensity of the LNMO peaks for all samples are increased from  $350^\circ\text{C}$  to  $750^\circ\text{C}$  and  $850^\circ\text{C}$ , respectively but decreased in intensity when the temperature reached  $950^\circ\text{C}$ . This is could be due to the decomposition of some LNMO particle at high temperature [22]. However, for LNMO prepared from acetate precursors, the peak intensities show high diffraction peaks and more crystalline than the LNMO powders synthesized from carbonate precursor. The sharp peak and high crystallinity of LNMO is important in the battery performances since it is beneficial for high discharge capacity and cycling stability [23]. In contrast, the intensity of the impurity peaks in Fig. 1 are smaller when compare with Fig. 2. The presence of impurity will block the mobility of  $\text{Li}^+$  in the structure, resulting in poor electrochemical performance [23]. Since low impurity content is giving a big impact to the electrochemical performance, LNMO powders synthesized from acetate precursors is at advantages in term of electrochemical performances.

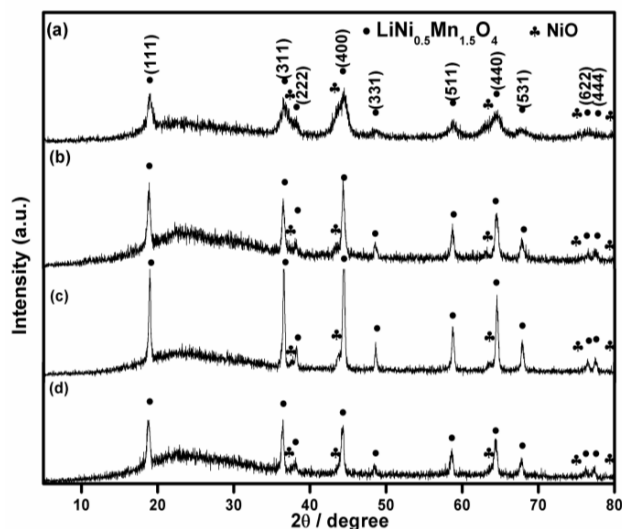


Fig. 1. XRD patterns of (a) A350, (b) A750, (c) A850 and (d) A950.

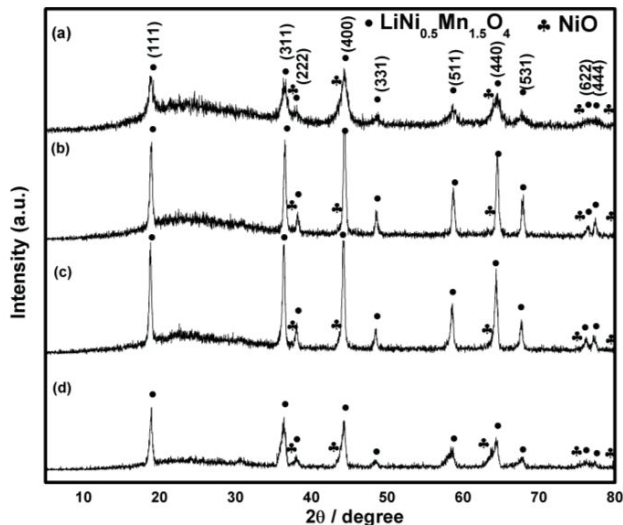


Fig. 2. XRD patterns of (a) C350, (b) C750, (c) C850 and (d) C950.

Fig. 3 shows the SEM images of LNMO synthesized from both precursors. Fig. 3 (a) and (b) show the samples formed large particles probably due to the low temperature applied during the annealing treatment. At the temperature of 850 °C (fig. 3 (c)), it can be seen that the size of the particles are ranging from ~ 1 to 4 μm , and at the temperature of 950 °C (fig. 3 (d)), the particles sizes increased up to ~ 3 to 5 μm with the formation of regular shape. On the other hand, the particles sizes in Fig. 3 (e) and (f) are much differ from the powders shown in Fig. 3 (a) and (b), which is about ~ 8 μm. The LNMO particles are clearly start to develop with polyhedral shape and smooth surface at the temperature of 850 °C (fig. 3 (g)) and exhibited larger particles sizes at the temperature of 950 °C. From Fig. 3 (d) and (h), the formation of polyhedral shape for Sample C950 could be due to the formation of well-faceted LNMO at high temperature while Sample A950 exhibits agglomeration and deformation of particles at elevated temperature [22].

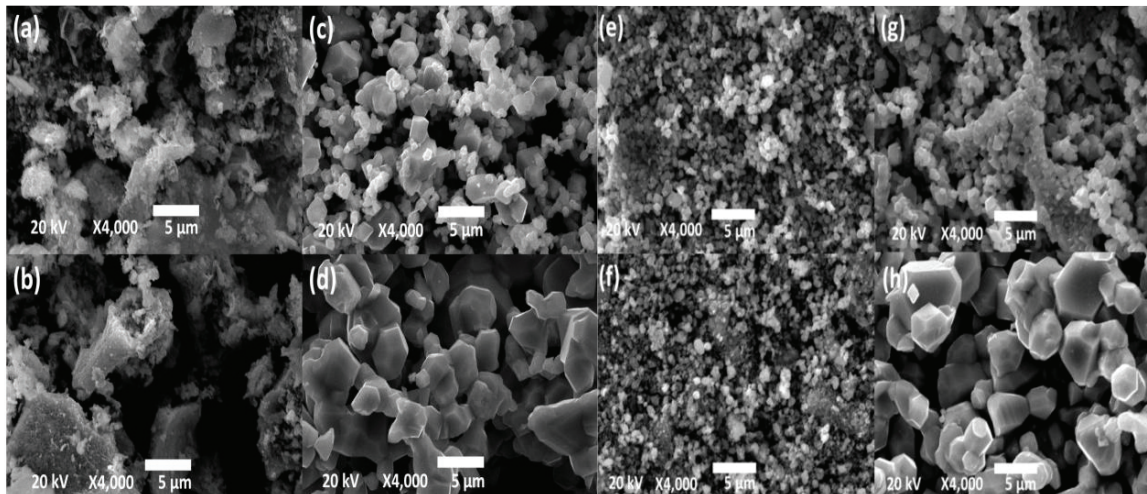


Fig. 3. SEM images of (a) A350, (b) A750, (c) A850, (d) A950, (e) C350, (f) C750 (g) C850 and (h) C950.

In general, the diffraction peaks intensities and crystallinity will give different electrochemical performance. Besides, smaller particle size could provide large surface area to a shorter path for  $\text{Li}^+$  ion diffusion and large specific active area for electrochemical reaction [23]. The electrochemical performances of LNMO synthesized from acetate precursors are shown in Fig. 4(a). Sample A750 shows the highest discharge capacity of  $120 \text{ mA h g}^{-1}$  at the 1<sup>st</sup> cycle, and capacity retention was about 92% when reach 100<sup>th</sup> cycle. However, sample A950 shows a better stability and cyclability when compare with sample A850. Although sample A850 delivered higher discharge capacity, the cyclability was further decreased with increasing cycle number. For sample A950, the discharge capacity was  $\sim 50 \text{ mAh g}^{-1}$  at the 1<sup>st</sup> cycle, and increased to  $\sim 80 \text{ mAh g}^{-1}$  at the 10<sup>th</sup> cycle. Then, the discharge capacity becomes steady for up to 100<sup>th</sup> cycle. The capacity retention of sample A950 are better than sample A850, this is might be due to the reaction between of the electrode and electrolyte during early cycle with the formation of solid electrolyte interphase (SEI) that cause low capacity of A950 [24]. Similar trends were observed in Fig. 4 (b). The increase in capacity upon cycling could be due to the activation and stabilization processes in the LNMO electrode [25]. The reason is that the morphological effects in the materials are expected to lead to diffusion limitations, and thus, the Li-ions might not be able to participate in the initial cycling. As the cycle number is increase, more active material may be able to contribute probably due to electrochemical grinding, which leads in increase capacity upon cycling [25, 26]. In Fig. 4 (b), sample C750 shows the highest discharge capacity of  $109 \text{ mAh g}^{-1}$  at the 1<sup>st</sup> cycle and exhibit capacity degradation. The capacity retention was calculated to be 87% when reach 100<sup>th</sup> cycle. Similar trend were demonstrated by sample C850 and C950 but with much lower discharge capacities.

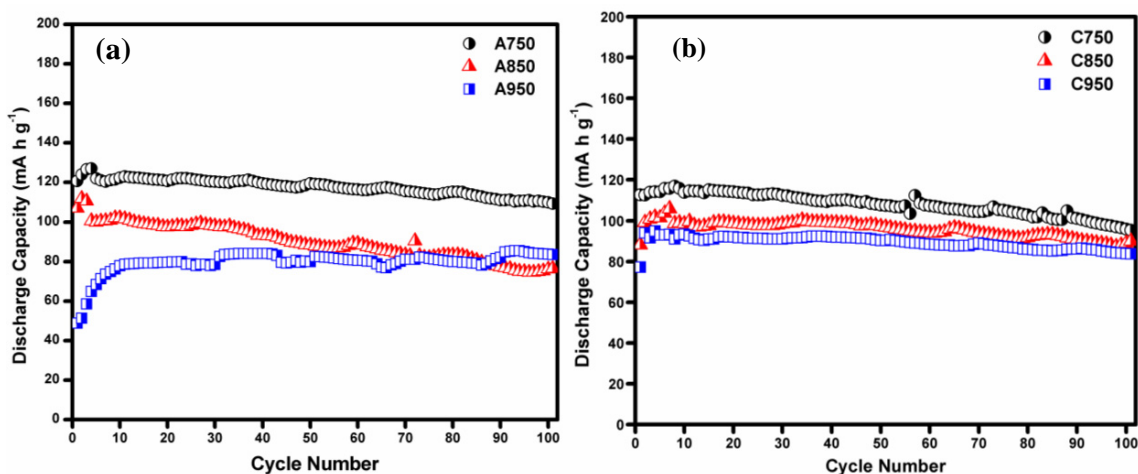


Fig. 4. The electrochemical performances of (a) A750, A850, and A950; and (b) C750, C850 and C950 at 1 C rate.

To further investigate the electrochemical properties of LNMO prepared from both precursors, cyclic voltammetry test was performed at a scan rate of  $0.5 \text{ mV s}^{-1}$ . From Fig. 5 (a) and (b), the redox reaction of sample A750, A850, A950, C750, C850, and C950 show similar peaks located near 4.70 and 4.75 V which can be attributed to redox couple of  $\text{Ni}^{2+}/\text{Ni}^{3+}$  and  $\text{Ni}^{3+}/\text{Ni}^{4+}$ , while peak located near 4.00 V are attribute to redox couple of  $\text{Mn}^{3+}/\text{Mn}^{4+}$  [22]. From Fig. 6 (a) and (b), both samples exhibit discharge capacity-voltage plateau at  $\sim 4.0$  and  $\sim 4.7$  V but with different magnitude which is in agreement with Fig. 5 (a) and (b). Clearly, these samples show a huge oxidation peak located at 4.0 V which ascribed to the large amount of  $\text{Mn}^{3+}$  ion. The large number of  $\text{Mn}^{3+}$  ion will cause poor cycling performances because  $\text{Mn}^{3+}$  is easy to disproportionate to  $\text{Mn}^{2+}$ . After passing through the separator,  $\text{Mn}^{2+}$  ions easily dissolve in electrolyte and capable to electrochemically depositing at anode surface that cause bad influence to the cycling performances [27]. Moreover, the initial charging capacity is high for both samples, indicating the formation of SEI and the electrolyte decomposition at high voltage, which produces a large capacity loss [24].

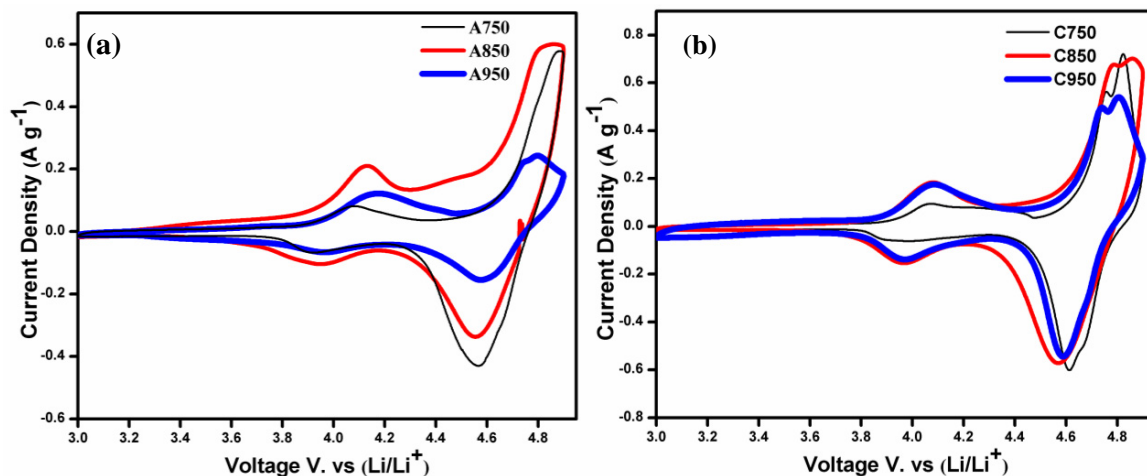


Fig. 5. Cyclic voltammograms of LNMO synthesized from (a) acetate and (b) carbonate precursors.

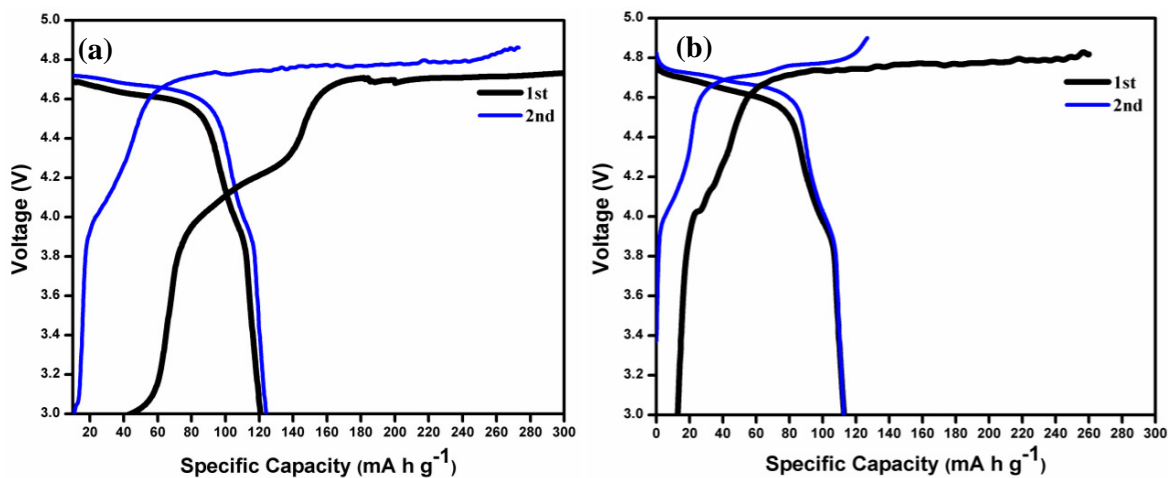


Fig. 6. Charge-discharge profile of (a) A750 and (b) C750 at 1 C rate.

From the above results, clearly that LNMO prepared from acetate precursor exhibits higher discharge capacity when compared with LNMO prepared from carbonate precursor. This could be due to the high crystallinity and small particle size of the samples, resulting from the presence of citric acid during the preparation process. Citric acid acts as a chelating agent during the synthesis process that could dissociate the ions and also help to fasten the decomposition of acetate ion, hence gives homogeneity to the LNMO samples [10]. The presence of NiO as an impurity could hinder the performances of the LNMO because it will block the path of  $\text{Li}^+$ . From the XRD and SEM, sample A750 shows a smaller intensity of impurity peaks and smaller particles sizes, therefore, the electrochemical performances of A750 is improved compared with other samples. Furthermore, Chi et al. [28] have shown that the lithium deficiency in the LNMO structure could be promoted when using acetate precursor when similar wet chemistry preparation is adopted by using nitrate precursor as reported by Reale et al. [29]. Hence, the used of acetate precursor shows an advantages than carbonate precursor.

#### 4. Conclusions

In summary, the LNMO synthesized from acetate and carbonate precursors with the addition of citric acid were successfully prepared using ball-milling method. The as-prepared LNMO materials were exhibited good crystallinity, regular shapes and smooth surfaces. The electrochemical properties of LNMO synthesized from acetate precursor exhibits better electrochemical performances in terms of capacity and cyclability. Clearly, the LNMO prepared from acetate precursor exhibit good electrochemical performances due to its solubility with the presence of citric acid, resulting in homogeneity of the solutions. Hence, these results could be useful for future work in order to solidify the research regarding enhancement of lithium-ion batteries.

#### Acknowledgement

Financial support was provided by the Ministry of Higher Education, Malaysia through a Fundamental Research Grant Scheme (FRGS) (Vote no. 59323) and MyBrain15 for the scholarships sponsored to the student is gratefully acknowledged.

#### References

- [1] K.S. Tan, M.V. Reddy, G.V.S. Rao, B.V.R. Chowdari, *Journal of Power Sources*. 147 (2005) 241-248.
- [2] J. Fu, Y. Bai, C. Liu, H. Yu, Y. Mo, *Materials Chemistry and Physics*. 115 (2009) 105-109.
- [3] G.H. Waller, S.Y. Lai, B.H. Rainwater, M. Liu, *Journal of Power Sources*. 251 (2014) 411-416.
- [4] Q. Wang, S. Deng, H. Wang, M. Xie, J. Liu, H. Yan, *Journal of Alloys and Compounds*. 553 (2013) 69-74.
- [5] C.J. Jafta, M.K. Mathe, N. Manyala, W.D. Roos, K.I. Ozoemena, *ACS applied materials & interfaces*. 5 (2013) 7592-7598.
- [6] X. Fang, C. Shen, M. Ge, J. Rong, Y. Liu, A. Zhang, F. Wei, C. Zhou, *Nano Energy*. 12 (2015) 43-51.
- [7] J. Chong, S. Xun, X. Song, G. Liu, V.S. Battaglia, *Nano Energy*. 2 (2013) 283-293.
- [8] M.V. Reddy, G.V. Subba Rao, B.V.R. Chowdari, *Chemical Reviews*. 113 (2013) 5364-5457.
- [9] Y.-L. Cui, Z. Sun, Q.-C. Zhuang, *Journal of Inorganic Organomet Polymer*. 21 (2011) 893-899.
- [10] N. Amdouni, K. Zaghbi, F. Gendron, A. Mauger, C.M. Julien, *Ionics*. 12 (2006) 117-126.
- [11] Z. Zhu, Qilu, D. Zhang, H. Yu, *Electrochimica Acta*. 115 (2014) 290-296.
- [12] S.-T. Myung, S. Komaba, N. Kumagai, H. Yashiro, H.-T. Chung, T.-H. Cho, *Electrochimica Acta*. 47 (2002) 2543-2549.
- [13] M.V. Reddy, H.Y. Cheng, J.H. Tham, C.Y. Yuan, H.L. Goh, B.V.R. Chowdari, *Electrochimica Acta*. 82 (2012) 269-275.
- [14] H. Wang, T.A. Tan, P. Yang, M.O. Lai, L. Lu, *The Journal of Physical Chemistry C*. 115 (2011) 6102-6110.
- [15] C. Locati, U. Lafont, L. Simonin, F. Ooms, E.M. Kelder, *Journal of Power Sources*. 174 (2007) 847-851.
- [16] M. Akkoulouch, J.M. Amarilla, R.M. Rojas, I. Saadoun, J.M. Rojo, *Journal of Power Sources*. 185 (2008) 501-511.
- [17] G.B. Zhong, Y.Y. Wang, Z.C. Zhang, C.H. Chen, *Electrochimica Acta*. 56 (2011) 6554-6561.
- [18] J.H. Kim, S.T. Myung, Y.K. Sun, *Electrochimica Acta*. 49 (2004) 219-227.
- [19] Y.-j. Hao, Q.-y. Lai, D.-q. Liu, Z.-u. Xu, X.-y. Ji, *Materials Chemistry and Physics*. 94 (2005) 382-387.
- [20] Z. Sheng-kui, W. You, L. Jie-qun, W. Jian, *Transactions of Nonferrous Metals Society of China*. 22 (2012) 2535-2540.
- [21] M. Shui, W. Zheng, J. Shu, Q. Wang, S. Gao, D. Xu, L. Chen, L. Feng, Y. Ren, *Current Applied Physics*. 13 (2013) 517-521.
- [22] Y.-Z. Lv, Y.-Z. Jin, Y. Xue, J. Wu, X.-G. Zhang, Z.-B. Wang, *Royal Society of Chemistry Advances*. 4 (2014) 26022-26029.
- [23] Y. Xue, Z. Wang, F. Yu, Y. Zhang, G. Yin, *Journal of Materials Chemistry A*. 2 (2014) 4185-4191.
- [24] L. Wang, H. Li, X. Huang, E. Baudrin, *Solid State Ionics*. 193 (2011) 32-38.
- [25] N.H. Idris, M.M. Rahman, J.-Z. Wang, Z.-X. Chen, H.-K. Liu, *Composites Science and Technology*. 71 (2011) 343-349.
- [26] A. Sakunthala, M.V. Reddy, S. Selvasekarapandian, B.V.R. Chowdari, H. Nithya, P.C. Selvin, *Journal of Solid State Electrochemistry*. 14 (2010) 1847-1854.
- [27] W.L. Jing Wang, Bihe Wu and Jinbao Zhao, *Journal of Materials Chemistry A*. 2 (2014) 16434-16442.
- [28] L.H. Chi, N.N. Dinh, S. Brutti, B. Scrosati, *Electrochimica Acta*. 55 (2010) 5110-5116.
- [29] P. Reale, S. Panero, B. Scrosati, *Journal of The Electrochemical Society*. 152 (2005) 1949-1954.